Biosensors and Bioelectronics 38 (2012) 74–78

Contents lists available at SciVerse ScienceDirect

Biosensors and Bioelectronics

journal homepage: www.elsevier.com/locate/bios

Monitoring protein–small molecule interactions by local pH modulation

Da Huang, Aaron D. Robison, Yiquan Liu, Paul S. Cremer*

Department of Chemistry, Texas A&M University, 3255 TAMU, College Station, TX 77843, United States

ARTICLE INFO

Article history:
Received 22 December 2011
Received in revised form
30 April 2012
Accepted 2 May 2012
Available online 6 June 2012

Keywords:
Biosensor
Fluorescein
Protein
Small molecule
pH sensitive
Labeling

ABSTRACT

We have developed a technique for sensing protein–small molecule and protein–ion interactions in bulk aqueous solution by utilizing a pH sensitive dye, 5-(and-6)-carboxyfluorescein, conjugated to free lysine residues on the surfaces of designated capture proteins. The fluorescein intensity was found to change by about 6% and 15% for small molecule and ion binding, respectively. The assay works by modulating the local electric fields around a pH sensitive dye. This, in turn, alters the dye's apparent pK_A value. Such changes may result directly from the charge on the analyte, occur through allosteric effects related to the binding process, or result from a combination of both. The assay was used to follow the binding of Ca^{2+} to calmodulin (CaM) and thiamine monophosphate (ThMP) to thiamine binding protein A (TbpA). The results demonstrate a binding constant of 1.1 μM for the Ca^{2+}/CaM pair and 3.2 nM for ThMP/TbpA pair, which are in excellent agreement with literature values. These assays demonstrate the generality of this method for observing the interactions of small molecules and ions with capture proteins. In fact, the assay should work as a biosensor platform for most proteins containing a specific ligand binding site, which would be useful as a simple and rapid preliminary screen of protein–ligand interactions.

1. Introduction

Measurements of the affinity of biomolecular interactions, such as protein–protein binding, protein–small molecule binding, and protein–ion binding not only provide insight into basic cellular processes but can also facilitate the development of therapeutics and serve as the basis for many diagnostic techniques (Bornhop et al., 2007). To date, numerous efforts have been made to monitor such ligand–receptor interactions. One potential drawback is that the devices associated with these techniques can be bulky, insensitive, and/or difficult to use. For example, calorimetric methods, such as isothermal titration calorimetry (ITC) (Leavitt and Freire, 2001; Velazquez Campoy and Freire, 2005; Wiseman et al., 1989), directly measure the heat associated with a given binding process. However, this method has relatively low sensitivity and usually requires large sample volumes. Moreover, it cannot be utilized if binding causes only very modest enthalpic changes. Interfacial methods, such as surface plasmon resonance (Hoffman et al., 2000; Li et al., 2008), microcantilever sensing (Raorane et al., 2008), and nanowire sensing (Zhang et al., 2010) permit detection down to the pM level and sometimes below it. Nevertheless, the requirement of immobilizing biomolecules onto surfaces can potentially cause problems. For example, the receptor sites on a protein might face the surface, inhibiting the binding process. Also, surface immobilization may influence the conformation and activity of the immobilized protein via partial or complete denaturation (Kerby et al., 2006).

Recently, Bornhop developed Back-Scattering Interferometry (BSI) to study biomolecular interactions in bulk solution (Bornhop et al., 2007). This method affords label-free ligand–receptor measurements with good sensitivity. It operates by exploiting the fringe patterns which are generated when a laser beam is shined onto a microfluidic channel in a direction perpendicular to the long axis of the channel. Shifts in the fringes arise when the refractive index of the solution inside the channel is changed. These shifts can be interpreted in terms of ligand–receptor binding with the aid of appropriate software.

Despite elegant advances such as BSI, there remains a pressing need to develop simple fluorescence-based techniques which can operate in bulk aqueous media. Indeed, fluorescence techniques can be sensitive down to the single molecule level (Jung et al., 2009; Lu et al., 1998; Xu et al., 2008) and are readily compatible with 96, 384, and 1536-well plate screening platforms (Boger et al., 2001; Kenaan et al., 2010; Mahendrarajah et al., 2011). Moreover, fluorescence assays are highly portable and can be used in conjunction with simple battery-operated, hand-held devices (Nelson et al., 2008). Efforts have been made to utilize fluorescence resonance energy transfer (FRET) techniques to study protein–ligand interactions or sense protein substrates (Mank et al., 2006; Nagl et al., 2008; Vaasa et al., 2010). However,

* Corresponding author. Tel.: +1 979 862 1200; fax: +1 979 845 7561.
E-mail address: cremer@mail.chem.tamu.edu (P.S. Cremer).

0956-5663/$ - see front matter © 2012 Elsevier B.V. All rights reserved.
http://dx.doi.org/10.1016/j.bios.2012.05.023

in order to obtain a FRET signal, two specially selected fluorescent dyes are required, one donor fluorophore and one acceptor fluorophore. These must be labeled on specific sites of the biomolecules (Mere et al., 1999; Sapsford et al., 2006), which can decrease the simplicity of such an approach.

Herein, we utilize a simple fluorescence-based biosensor assay which exploits a pH-sensitive fluorescent dye. The dye, 5-(and-6)-carboxyfluorescein, is strongly fluorescent at high pH values and less fluorescent at low pH (Mordon et al., 1992). Moreover, this dye is sensitive to factors which can influence the local chemical environment, such as changes in the local dielectric constant or local electric fields. The physical principle for this method is based on the idea that the pH sensitive probe can be placed in proximity to a protein binding pocket by conjugation to free lysine residues via succinimidyl ester-linkages. The apparent pK_A of the dye will be modulated when charged ligands bind or through rearrangements due to allosteric effects. A schematic illustration of this concept is shown in Fig. 1. In the example, a capture protein (shown in orange) is conjugated with fluorescein dyes. These fluorophores initially have relatively strong fluorescence, which decreases upon the binding of a target ligand (shown in purple). In this rendition, the platform is a "turn off" sensor. This can be the case if the target ligand is negatively charged at the operating pH as this will recruit hydronium ions around the capture protein and, therefore, help protonate the fluorescein probe. Alternatively, if the target ligand induces a conformational change to the protein upon binding, this too may influence the local chemical environment and consequently modulate the intensity of the dye.

In order for the present method to be effective, the pH sensitivity of the fluorescent probe should fall within the region of interest for measuring ligand–receptor attachment. A simple choice is 5-(and 6-) carboxyfluorescein, which has its largest fluorescence variation between pH 6.0 and pH 7.4 (Mordon et al., 1992). As the dye molecule is deprotonated, its fluorescence is "turned on". Thus, this dye is an excellent reporter candidate for many biomolecular interaction assays. Indeed, labeling with fluorescein has been utilized as a pH sensor to monitor protein–protein interactions with good results (Lavis et al., 2007). In addition, protein folding processes and even protein conformational changes have been studied with the help of fluorescein labeling (Garel, 1976; Goldberg and Baldwin, 1998; Griep and McHenry, 1990; Labhardt et al., 1983). Although the success and relative simplicity of these fluorescein-based biomolecular assays has been shown for protein folding and protein–protein interactions, to date there have been no investigations of similar strategies for small molecule and ion sensing. This is unfortunate, as a simple dye-attachment assay could be used to rapidly screen ligand–receptor binding in preliminary experiments before putative targets are further explored by more labor intensive methods.

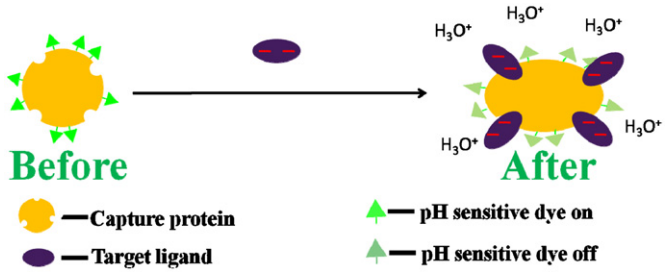

Fig. 1. Schematic diagram illustrating the principles of a pH-sensitive dye acting as a reporter for a protein–ligand binding process. (Before) In the absence of the target protein, the dye molecules conjugated to the capture protein are in the "on state". (After) Upon binding the target ligand, the negatively charged target ligands recruit hydronium ions and decrease the apparent local pH around the protein as well as possibly cause a conformational change. As a result, the dye molecules on the capture protein are turned off. (For interpretation of the references to color in this figure, the reader is referred to the web version of this article.)

Herein, we demonstrate the use of fluorescein as a local pH sensor on proteins for monitoring the interaction of small molecules and ions, specifically observing thiamine monophosphate (ThMP) with thiamine binding protein A (TbpA), and Ca^{2+} with calmodulin (CaM). This platform is quite versatile and appears to be generically useful for monitoring protein–ion and protein–small molecule interactions.

2. Experimental section

2.1. Materials

(5-and-6)-carboxyfluorescein, succinimidyl esters (mixed isomers) (5(6)-FAM-SE) were purchased from Invitrogen (Carlsbad, CA). Bovine calmodulin and thiamine monophosphate were purchased from Sigma-Aldrich (St. Louis, MO). Thiamine binding protein A was supplied by the Begley laboratory at TAMU. Bio-Spin columns with Bio-Gel P-6 were obtained from Bio-Rad (Hercules, CA) and purified water was produced from a NANOpure Ultrapure Water System (18.2 MΩ cm, Barnstead, Dubuque, IA).

2.2. Protein labeling procedure

TbpA solutions were made with 10 mM phosphate buffered saline (PBS) at pH 7.2 and a protein concentration of 2 mg/ml. The buffer contained 150 mM NaCl and 1 mM NaN_3. To label the proteins, 20 μL of 1 M Na_2CO_3 was added to 100 μL of a 2 mg/ml protein solution. Next, 0.3 mg of 5(6)-FAM-SE were added to the solution and stored at 4 °C for 2 days. Subsequently, the labeled proteins were separated from remaining free dye molecules via Bio-Spin columns with Bio-Gel P-6.

Calmodulin was reconstituted from a lyophilized powder by 50 mM HEPES buffer containing 150 mM NaCl and 1 mM EGTA to a final concentration of 2 mg/ml. 5 μL of 1 M Na_2CO_3 and 1 μL of 10 mg/ml 5(6)-FAM-SE DMSO solution were sequentially added to a 50 μL calmodulin solution. The solution was then stored at 4 °C overnight. Finally, remaining free dye was separated from the labeled protein with a Bio-Spin column before use.

2.3. pH titration curve measurements

100 mM Tris/Citrate buffer was prepared at pH values ranging from 4.0 to 6.5 by adjusting the pH with NaOH/HCl. 100 mM Tris buffer was prepared at pH values ranging from 7.0 to 11.0 by adjusting the pH with NaOH/HCl. These pH values were chosen to locate the pK_A value of the fluorescein dye conjugated to each protein. The pH was obtained with a standard glass electrode setup with measurements having an error of ± 0.1 pH units. Titration curves for the dye molecules on the proteins were made by adding 5 μL of a fluorescein-labeled protein solution to 95 μL of buffer. Fluorescence emission spectra were obtained by a QE 65000-FL Scientific Grade Spectrometer (Ocean Optics, Dunedin, FL) by setting the excitation peak to 488 nm.

2.4. Protein concentration and DOL (degree of labeling)

The absorbance of fluorescein labeled proteins was determined at pH 8.0 in 100 mM Tris buffer. Measurements were made using an Agilent 8452 UV–visible Spectrophotometer (Lexington, MA). The concentration of dye was determined via the Beer–Lambert law and the degree of labeling (*DOL*) was obtained by the following equation: $DOL = C_{dye}/C_{protein}$, where C_{dye} and

$C_{protein}$ are the solution concentrations of the respective species. The extinction coefficient at 494 nm used for fluorescein was 68,000 M^{-1}, which was provided by Invitrogen. The DOL values for the proteins employed herein are: 9.7 for TbpA and 1.5 for CaM. Increasing this degree of labeling could improve sensitivity, but is likely to also interfere with ligand–receptor binding or cause changes in structure.

2.5. Binding measurements

For fluorescein-labeled TbpA binding to ThMP, 1 μL of 1.67 mg/ml dye-labeled TbpA was added to 2 ml of 100 mM Tris/50 mM citrate buffer at pH 6.5 in a QVFL-Q-10 cuvette. In this case, aliquots of 25 μM ThMP in water were added to the cuvette to generate different concentrations of ThMP with a 15 min room temperature incubation allowed before each measurement. For fluorescein-labeled CaM binding to Ca^{2+}, 6 μL of 1.54 mg/ml 5(6)-FAM labeled CaM was added to 94 μL of 50 mM HEPES buffer containing 150 mM NaCl and 1 mM EGTA at pH 6.8 in a type 703 M cuvette (Precision Cell, Farmingdale, NY). Aliquots of either 10 mM or 100 mM $CaCl_2$ were introduced stepwise to generate different free Ca^{2+} concentrations with a 1 min incubation period at 25 °C allowed before each measurement. All fluorescence emission spectra were obtained with a QE 65000-FL Scientific Grade Spectrometer by setting the excitation peak to 488 nm.

Error analysis of the emission intensity was performed. The fluorescence intensity of labeled TbpA protein diluted in buffer solution in a cuvette was found to be stable to within 0.4% over 10 min of continuous excitation in the fluorometer. In another control, ThMP was introduced into a solution of TbpA and free dye, which led to almost no signal change. Moreover, 100 nM biotin and 100 nM adenosine monophosphate (AMP) molecules, respectively, were introduced to a labeled TbpA solution. This gave rise to no signal changes, indicating that fluorescence modulation was selective to the specific target molecule.

CaM–Ca^{2+} binding measurements described herein have been accompanied by control experiments that utilized free dye in solution instead of labeled proteins to establish that the signal was indeed due to the putative binding event rather than changes in fluorescence caused by dye–analyte interactions. Almost no signal changes were observed in the presence of ThMP. For Ca^{2+}, the control assays gave rise to an approximately 1% intensity decrease in fluorescence at the highest Ca^{2+} concentration employed. This change was probably due to a slight decrease in the bulk pH rather than any direct Ca^{2+}-fluorescence interaction. In fact, the change was linear with pH and could easily be distinguished from the Langmuir isotherm response due to CaM–Ca^{2+} interactions.

3. Results

3.1. Titration curves for fluorescein-labeled proteins

In a first set of experiments, titration curves of fluorescence intensity vs. solution pH were obtained for fluorescein conjugated to TbpA and CaM. The experiments were performed by using solutions of varying pH ranging from acidic to basic. Fluorescence spectra obtained at multiple pH values are provided in Fig. 2. As expected, the conjugated dye molecules showed higher florescence intensity at more basic pH values and lower intensity at relatively acidic pH. The titration curves were not strongly influenced by the specific protein to which the dyes were attached. The apparent pK_A value was 6.4 ± 0.1 for both TbpA and CaM.

3.2. Binding curve for TbpA and ThMP

TbpA is the thiamine periplasmic-binding protein from *E. coli* (Hollenbach et al., 2002), which has been shown to bind ThMP with modestly high affinity, having a reported K_d around 2.3 nM (Soriano et al., 2008). The acidic phosphate group on the ThMP molecule brings down the local pH around the binding site of TbpA, thus making the binding of ThMP to TbpA observable via the fluorescence intensity decrease of dye-labeled TbpA. The assay pH was chosen to be 6.5, which is located just above the middle of the slope in Fig. 2a. TbpA and ThMP bind in a 1 to 1 ratio and a Langmuir isotherm could be employed to fit the data for the titration curve in Fig. 3a according to Eq. (1):

$$[\mathrm{ThMP}]_0 = k \times \delta F + \frac{K_d \times k \times \delta F}{[\mathrm{TbpA}]_0 - k \times \delta F} \quad (1)$$

It should be noted that this equation differs from a standard Langmuir isotherm made with a surface containing immobilized receptor sites in contact with a bulk liquid. That is because the liquid can typically be flowed over the surface continuously until equilibrium is achieved. By contrast, in bulk solution one has a fixed number of TbpA proteins and these are titrated with ThMP. As such, only the added amount of ThMP is controlled and some of these molecules are bound while the rest are unbound. In this case, it is assumed that the fluorescence change should be directly related to the formation of the TbpA–ThMP complex (Eq. (2)):

$$[\mathrm{ThMP{-}TbpA}] = k \times \delta F \quad (2)$$

Here [ ] denotes concentration, k is a constant representing the intrinsic relationship between the relative fluorescence change and the TbpA–ThMP complex concentration, and δF is the relative fluorescence change $|1-F/F_0|$,where F and F_0 indicate the final and initial integrated average fluorescence intensity from 520 nm to 530 nm, respectively. According to the definition of the

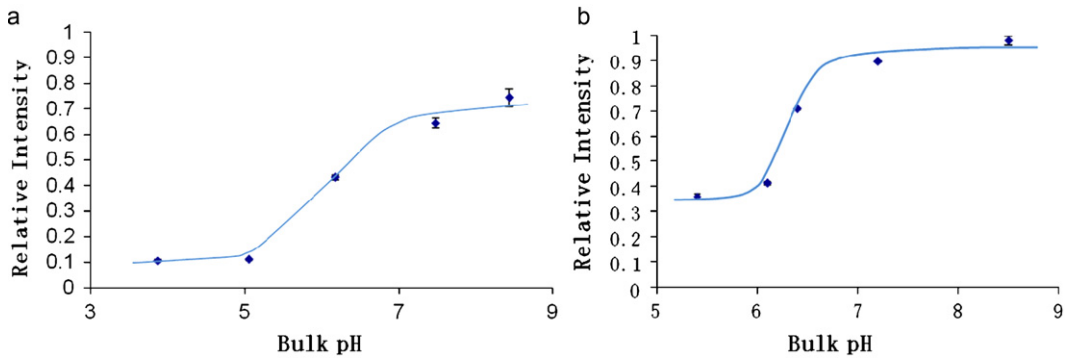

Fig. 2. Relative fluorescence intensity of fluorescein-conjugated proteins as a function of pH for 2 different proteins: (a) TbpA and (b) CaM. The blue lines represent guides to the eye for the titration curves. (For interpretation of the references to color in this figure legend, the reader is referred to the web version of this article.)

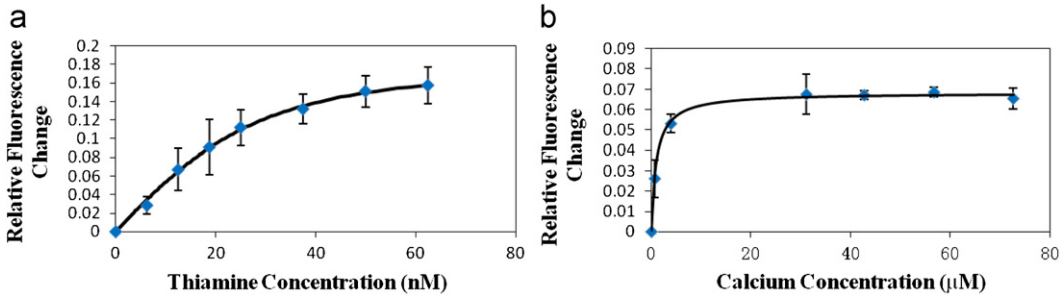

Fig. 3. Plots of the relative fluorescence intensity change ($|1-F/F_0|$) vs. substrate concentration for two labeled protein–substrate binding systems. Each data point represents the average of three measurements and the error bars are standard deviations from those measurements. The solid curves through the data are the best fits to Eqs. (4) and (6). (a) The plot for the fluorescein-labeled TbpA/ThMP pair. (b) The plot for the fluorescein-labeled CaM/Ca^{2+} pair.

Table 1
Summary of K_d values found here and literature values.

Binding partners	Measured K_d values	Literature K_d values	Detection method of published data
Labeled TbpA–ThMP	3.2 nM	2.3 nM	Intrinsic protein fluorescence measurement (Soriano et al., 2008)
Labeled CaM–Ca^{2+}	1.1 μM	1–10 μM	Equilibrium and flow dialysis (Tsuruta and Sano, 1990).

dissociation constant, one can write (Eq. (3)):

$$[\text{TbpA}-\text{ThMP}] = ([\text{TbpA}]_0 - [\text{TbpA}-\text{ThMP}])([\text{TbpA}-\text{ThMP}])/K_d \quad (3)$$

where $[\ ]_0$ denotes the initial concentration or added concentration. Combining Eqs. (1) and (2) generates an equation describing the relation of relative fluorescence intensity change and ThMP concentration (Eq. (4)):

$$[\text{ThMP}] = k \times \delta F + \frac{K_d \times k \times \delta F}{[\text{TbpA}] - k \times \delta F} \quad (4)$$

The extracted dissociation constant of 3.2 ± 0.7 nM matches well with the literature value and the detection limit for ThMP is 2.1 nM. This assay provides direct evidence that our method is capable of following small molecule–protein binding events.

3.3. Binding curve for CaM with Ca^{2+}

CaM, the ubiquitous Ca^{2+} binding protein, was chosen to demonstrate the ability of this method to follow protein–ion interactions. It is known that this protein can bind to and regulate a multitude of different protein targets (Bornhop et al., 2007; Klee et al., 1980). Most studies have suggested that CaM contains either multiple classes of binding sites for Ca^{2+} or negative cooperativity (Klee, 1977; Lin et al., 1974; Teo and Wang, 1973). Literature K_d values for CaM–Ca^{2+} binding vary from 1 to 10 μM (Bornhop et al., 2007; Tsuruta and Sano, 1990). In the current assay, the operating pH was 6.8, which is at the top of the linear range of the titration curve (Fig. 2b). Interestingly, the binding of Ca^{2+} to CaM leads to a decrease in fluorescence signal, which indicates that the charge on the cation is not the dominant factor in changing the fluorescence response of the dye. CaM contains eight lysine residues, three of which are located within Ca^{2+} binding domains and one of which is C-terminally located (Zhang et al., 1995). This C-terminal lysine is well exposed to solution and should be readily labeled by the dye. Crystal structure analysis in the presence and absence of Ca^{2+} show that this residue undergoes a conformational shift, which may result in a decrease in fluorescence intensity. The binding curve is shown in Fig. 3b. Note that EGTA is added to the buffer to help maintain the free Ca^{2+} concentration at a constant level (Qin et al., 1999). The data are modeled using a Langmuir isotherm fit (Eq. (5)):

$$\text{Bound sites} = \frac{[\text{Ca}^{2+}]}{K_d + [\text{Ca}^{2+}]} \quad (5)$$

Next, the relative fluorescence change from this binding process can be designated as δF. A constant, k, is needed to relate δF to CaM–Ca^{2+} complex formation. From these, an equation describing the relationship between the relative fluorescence intensity change and Ca^{2+} concentration can be written as (Eq. (6))

$$\delta F = \frac{[\text{Ca}^{2+}]}{K_d + [\text{Ca}^{2+}]} \times \frac{1}{k} \quad (6)$$

The abstracted equilibrium dissociation constant was 1.1 ± 0.07 μM and the detection limit for Ca^{2+} was 0.16 μM. The dissociation constant values measured for the two processes described above along with literature values are summarized in Table 1.

4. Discussion

4.1. Assay sensitivity and the advantages of random labeling

We have developed a pH dependent assay for monitoring protein/substrate binding in bulk solution. This method is quite general as the assay can be employed for protein–small molecule and protein–ion binding in a similar fashion. As long as ligand binding sites affect a region located within the Debye length of the pH sensitive dye, the protein-conjugated fluorophore will be directly sensitive to the binding of the ligand. Under physiological conditions (about 100 mM salt), the Debye length is typically on the order of 1–2 nm (Israelachvili, 1985). Therefore, each conjugated dye will work as a local sensor that investigates the pH over a few square nanometers of protein surface area. The interaction of a ligand with the binding pocket of a protein will modulate the protonation of D, E, K, R, and H residues as well as possibly cause the protein to undergo conformational changes. All of these effects can ultimately influence the local electric fields in the vicinity of the fluorescent probe.

A key choice in our method is the decision to use random labeling, which attaches dye molecules to free lysine residues on each protein. Such random labeling will result in some dye molecules that are far away from the protein binding pocket as

well as others nearer to the interaction site. This may generate background signal, which can lower the sensitivity of the assay compared to site-specific labeling techniques (Hanes et al., 2011). However, site-specific labeling requires significantly more work that is better suited to studying particular protein–ligand interaction pairs in great detail. Random labeling affords the ability to perform many preliminary assays to rapidly screen putative protein–ligand interactions, such as sorting out the right class of substrate for various enzymes, before embarking on the use of more time consuming and costly characterization techniques.

4.2. Development of heterogeneous vs. homogeneous assays

Previously, we have developed a heterogeneous pH modulation assay for monitoring the binding of proteins to planar supported lipid bilayers at the liquid/solid interface (Jung et al., 2009). In that case, ligands as well as the pH sensitive dye, *ortho*-Texas Red, were embedded into a membrane via conjugation to lipid head groups. The choice of the fluorescent dye employed in the heterogeneous assay was highly restricted because of the need to have an extremely photostable dye at the solid/liquid interface. By contrast, a potentially much wider variety of pH sensitive dyes can be employed in bulk solution assays as photobleaching is not such a serious problem in that case. Indeed, the light intensity required in bulk solution is much lower because many more dye molecules are present in the beam path. Another key difference in the case of the homogeneous assays explored herein is the ability to use a simple fluorimeter instead of a cooled CCD camera for detecting the signal. Of course, the same type of direct dye-conjugated protein assay developed here could also be run as a heterogeneous assay. In that case, careful preparation of the surface would be required to circumvent problems related to protein orientation and denaturation.

5. Conclusion

In summary, the pH modulation technique developed in this study for bulk solution assays is a simple, sensitive, and highly versatile screening technique, and though it does not give the optimized signal of site-specific labeling, is useful for preliminary studies involving protein–substrate interactions in bulk solution. The technique only requires one simple labeling step, as opposed to Förster resonance energy transfer (FRET) techniques, which require labeling of two fluorescent dyes at specific locations. Also, this method utilizes a fluorimeter, which is commonly available in many laboratories. Finally, different pH ranges can be accessed, if desired, by using a variety of pH sensitive dye molecules (e.g. pHrodo, rhodamine red, coumarin dyes, *ortho*-Texas Red, or Oregon Green).

Acknowledgments

This work was funded by the Office of Naval Research (Grant no. N00014-08-1-0467).

References

Boger, D.L., Fink, B.E., Brunette, S.R., Tse, W.C., Hedrick, M.P., 2001. Journal of the American Chemical Society 123 (25), 5878–5891.
Bornhop, D.J., Latham, J.C., Kussrow, A., Markov, D.A., Jones, R.D., Sorensen, H.S., 2007. Science (Washington DC, US) 317 (5845), 1732–1736.
Garel, J.R., 1976. European Journal of Biochemistry 70 (1), 179–189.
Goldberg, J.M., Baldwin, R.L., 1998. Biochemistry 37 (8), 2546–2555.
Griep, M.A., McHenry, C.S., 1990. Journal of Biological Chemistry 265 (33), 20356–20363.
Hanes, J.W., Chatterjee, D., Soriano, E.V., Ealick, S.E., Begley, T.P., 2011. Chemical Communications 47 (8), 2273–2275.
Hoffman, T.L., Canziani, G., Jia, L., Rucker, J., Doms, R.W., 2000. Proceedings of the National Academy of Sciences of the United States of America 97 (21), 11215–11220.
Hollenbach, A.D., Dickson, K.A., Washabaugh, M.W., 2002. Protein Expression and Purification 25 (3), 508–518.
Israelachvili, J.N., 1985. Intermolecular and Surface Forces: With Applications to Colloidal and Biological Systems. Academic Press, London; Orlando Fla.
Jung, H., Robison, A.D., Cremer, P.S., 2009. Journal of the American Chemical Society 131 (3), 1006–1014.
Kenaan, C., Zhang, H., Hollenberg, P.F., 2010. Nature Protocols 5 (10), 1652–1658.
Kerby, M.B., Legge, R.S., Tripathi, A., 2006. Analytical Chemistry 78 (24), 8273–8280.
Klee, C.B., 1977. Biochemistry 16 (5), 1017–1024.
Klee, C.B., Crouch, T.H., Richman, P.G., 1980. Annual Review of Biochemistry 49, 489–515.
Labhardt, A.M., Ridge, J.A., Lindquist, R.N., Baldwin, R.L., 1983. Biochemistry 22 (2), 321–327.
Lavis, L.D., Rutkoski, T.J., Raines, R.T., 2007. Analytical Chemistry 79 (17), 6775–6782.
Leavitt, S., Freire, E., 2001. Current Opinion in Structural Biology 11 (5), 560–566.
Li, Y.C., Chang, Y.F., Su, L.C., Chou, C., 2008. Analytical Chemistry 80 (14), 5590–5595.
Lin, Y.M., Liu, Y.P., Cheung, W.Y., 1974. Journal of Biological Chemistry 249 (15), 4943–4954.
Lu, H.P., Xun, L., Xie, X.S., 1998. Science (Washington DC, US) 282 (5395), 1877–1882.
Mahendrarajah, K., Dalby, P.A., Wilkinson, B., Jackson, S.E., Main, E.R., 2011. Analytical Biochemistry 411 (1), 155–157.
Mank, M., Reiff, D.F., Heim, N., Friedrich, M.W., Borst, A., Griesbeck, O., 2006. Biophysical Journal 90 (5), 1790–1796.
Mere, L., Bennett, T., Coassin, P., England, P., Hamman, B., Rink, T., Zimmerman, S., Negulescu, P., 1999. Drug Discovery Today 4 (8), 363–369.
Mordon, S., Maunoury, V., Devoisselle, J.M., Abbas, Y., Coustaud, D., 1992. Journal of Photochemistry and Photobiology, B 13 (3–4), 307–314.
Nagl, S., Bauer, R., Sauer, U., Preininger, C., Bogner, U., Schaeferling, M., 2008. Biosensors and Bioelectronics 24 (3), 397–402.
Nelson, N., Sander, D., Dandinf, M., Sarje, A., Prakash, S., Ji, H.H., Abshire, P., 2008. In: Proceedings of the IEEE International Symposium on Circuits and Systems (ISCAS), Seattle, pp. 1080–1083.
Qin, N., Olcese, R., Bransby, M., Lin, T., Birnbaumer, L., 1999. Proceedings of the National Academy of Sciences of the United States of America 96 (5), 2435–2438.
Raorane, D.A., Lim, M.D., Chen, F.F., Craik, C.S., Majumdar, A., 2008. Nano Letters 8 (9), 2968–2974.
Sapsford, K.E., Berti, L., Medintz, I.L., 2006. Angewandte Chemie-International Edition 45 (28), 4562–4589.
Soriano, E.V., Rajashankar, K.R., Hanes, J.W., Bale, S., Begley, T.P., Ealick, S.E., 2008. Biochemistry 47 (5), 1346–1357.
Teo, T.S., Wang, J.H., 1973. Journal of Biological Chemistry 248 (17), 5950–5955.
Tsuruta, H., Sano, T., 1990. Biophysical Chemistry 35 (1), 75–84.
Vaasa, A., Lust, M., Terrin, A., Uri, A., Zaccolo, M., 2010. Biochemical and Biophysical Research Communications 397 (4), 750–755.
Velazquez Campoy, A., Freire, E., 2005. Biophysical Chemistry 115 (2–3), 115–124.
Wiseman, T., Williston, S., Brandts, J.F., Lin, L.N., 1989. Analytical Biochemistry 179 (1), 131–137.
Xu, W., Kong, J.S., Yeh, Y.T., Chen, P., 2008. Nature Materials 7 (12), 992–996.
Zhang, G.J., Huang, M.J., Luo, Z.H., Tay, G.K., Lim, E.J., Liu, E.T., Thomsen, J.S., 2010. Biosensors and Bioelectronics 26 (2), 365–370.
Zhang, M., Tanaka, T., Ikura, M., 1995. Nature Structural & Molecular Biology 2 (9), 758–767.